

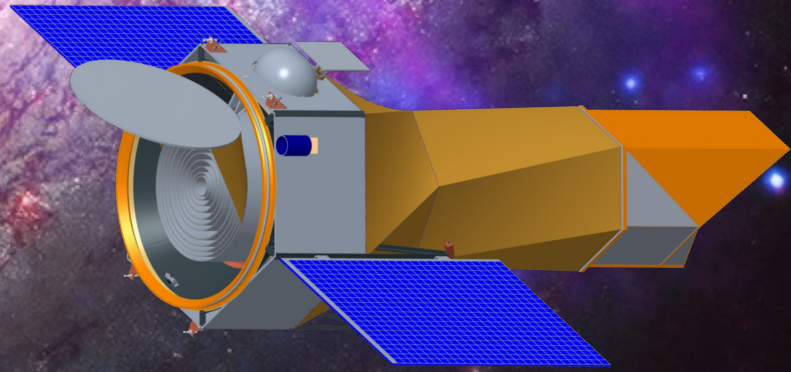
# Line Emission Mapper



Probing the physics of cosmic ecosystems

astro-ph.IM] 13 Apr 2023

arXiv:2211.09827v4



A mission concept for the NASA 2023 Astrophysics Probes AO

Ralph Kraft<sup>1</sup>, Maxim Markevitch<sup>2</sup>, Caroline Kilbourne<sup>2</sup>, Joseph S. Adams<sup>2</sup>, Hiroki Akamatsu<sup>3</sup>,  
Mohammadreza Ayromlou<sup>4</sup>, Simon R. Bandler<sup>2</sup>, Marco Barbera<sup>51,52</sup>, Douglas A. Bennett<sup>5</sup>, Anil Bhardwaj<sup>6</sup>,  
Veronica Biffi<sup>7</sup>, Dennis Bodewits<sup>8</sup>, Ákos Bogdán<sup>1</sup>, Massimiliano Bonamente<sup>9</sup>, Stefano Borgani<sup>7</sup>,  
Graziella Branduardi-Raymont<sup>10</sup>, Joel N. Bregman<sup>11</sup>, Joseph N. Burchett<sup>12</sup>, Jenna Cann<sup>2</sup>, Jenny Carter<sup>13</sup>,  
Priyanka Chakraborty<sup>1</sup>, Eugene Churazov<sup>14,15</sup>, Robert A. Crain<sup>16</sup>, Renata Cumbee<sup>2</sup>, Romeel Davé<sup>17</sup>,  
Michael DiPirro<sup>2</sup>, Klaus Dolag<sup>18</sup>, W. Bertrand Doriese<sup>5</sup>, Jeremy Drake<sup>1</sup>, William Dunn<sup>10</sup>, Megan Eckart<sup>19</sup>,  
Dominique Eckert<sup>20</sup>, Stefano Ettori<sup>32</sup>, William Forman<sup>1</sup>, Massimiliano Galeazzi<sup>21</sup>, Amy Gall<sup>1</sup>, Efrain Gatuzz<sup>22</sup>,  
Natalie Hell<sup>19</sup>, Edmund Hodges-Kluck<sup>2</sup>, Caitriona Jackman<sup>23</sup>, Amir Jahromi<sup>2</sup>, Fred Jennings<sup>17</sup>, Christine Jones<sup>1</sup>,  
Philip Kaaret<sup>24</sup>, Patrick J. Kavanagh<sup>23</sup>, Richard L. Kelley<sup>2</sup>, Ildar Khabibullin<sup>18,14</sup>, Chang-Goo Kim<sup>25</sup>,  
Dimitra Koutroumpa<sup>26</sup>, Orsolya Kovács<sup>27</sup>, K. D. Kuntz<sup>28</sup>, Erwin Lau<sup>1</sup>, Shiu-Hang Lee<sup>30</sup>, Maurice Leutenegger<sup>2</sup>,  
Sheng-Chieh Lin<sup>29</sup>, Carey Lisse<sup>31</sup>, Ugo Lo Cicero<sup>52</sup>, Lorenzo Lovisari<sup>32,1</sup>, Dan McCammon<sup>33</sup>, Seán McEntee<sup>23</sup>,  
François Mernier<sup>2,36</sup>, Eric D. Miller<sup>34</sup>, Daisuke Nagai<sup>35</sup>, Michela Negro<sup>2,37</sup>, Dylan Nelson<sup>4</sup>, Jan-Uwe Ness<sup>38</sup>,  
Paul Nulsen<sup>1</sup>, Anna Ogorzałek<sup>2,36</sup>, Benjamin D. Oppenheimer<sup>39</sup>, Lidia Oskinova<sup>40</sup>, Daniel Patnaude<sup>1</sup>,  
Ryan W. Pfeifle<sup>2</sup>, Annalisa Pillepich<sup>41</sup>, Paul Plucinsky<sup>1</sup>, David Pooley<sup>42</sup>, Frederick S. Porter<sup>2</sup>, Scott Randall<sup>1</sup>,  
Elena Rasia<sup>7</sup>, John Raymond<sup>1</sup>, Mateusz Ruszkowski<sup>11,14</sup>, Kazuhiro Sakai<sup>2</sup>, Arnab Sarkar<sup>34</sup>, Manami Sasaki<sup>43</sup>,  
Kosuke Sato<sup>44</sup>, Gerrit Schellenberger<sup>1</sup>, Joop Schaye<sup>45</sup>, Aurora Simionescu<sup>3,45,46</sup>, Stephen J. Smith<sup>2</sup>,  
James F. Steiner<sup>1</sup>, Jonathan Stern<sup>47</sup>, Yuanyuan Su<sup>29</sup>, Ming Sun<sup>9</sup>, Grant Tremblay<sup>1</sup>, Nhut Truong<sup>41</sup>, James Tutt<sup>48</sup>,  
Eugenio Ursino<sup>53</sup>, Sylvain Veilleux<sup>36</sup>, Alexey Vikhlinin<sup>1</sup>, Stephan Vladutescu-Zopp<sup>18</sup>, Mark Vogelsberger<sup>34</sup>,  
Stephen A. Walker<sup>9</sup>, Kimberly Weaver<sup>2</sup>, Dale M. Weigt<sup>23</sup>, Jessica Werk<sup>49</sup>, Norbert Werner<sup>27</sup>, Scott J. Wolk<sup>1</sup>,  
Congyao Zhang<sup>50</sup>, William W. Zhang<sup>2</sup>, Irina Zhuravleva<sup>50</sup>, John ZuHone<sup>1</sup>

*Draft mission concept, March 2023*

- <sup>1</sup> Center for Astrophysics | Harvard & Smithsonian
- <sup>2</sup> NASA Goddard Space Flight Center
- <sup>3</sup> SRON, the Netherlands
- <sup>4</sup> Universität Heidelberg, Germany
- <sup>5</sup> NIST, Boulder, Colorado
- <sup>6</sup> Physical Research Laboratory, Ahmedabad, India
- <sup>7</sup> INAF, Trieste, Italy
- <sup>8</sup> Auburn University, Auburn, Alabama
- <sup>9</sup> University of Alabama, Huntsville
- <sup>10</sup> University College London, U.K.
- <sup>11</sup> University of Michigan
- <sup>12</sup> New Mexico State University
- <sup>13</sup> Leicester University, UK
- <sup>14</sup> MPA, Garching, Germany
- <sup>15</sup> IKI, Moscow, Russia
- <sup>16</sup> Liverpool John Moores University, U.K.
- <sup>17</sup> University of Edinburgh, U.K.
- <sup>18</sup> Ludwig-Maximilians-Univ. München, Germany
- <sup>19</sup> LLNL
- <sup>20</sup> University of Geneva, Switzerland
- <sup>21</sup> University of Miami, Florida
- <sup>22</sup> MPE, Garching, Germany
- <sup>23</sup> DIAS, Dublin, Ireland
- <sup>24</sup> University of Iowa
- <sup>25</sup> Princeton University
- <sup>26</sup> LATMOS, CNRS, France
- <sup>27</sup> Masaryk University, Brno, Czech Republic
- <sup>28</sup> Johns Hopkins University
- <sup>29</sup> University of Kentucky
- <sup>30</sup> Kyoto University, Japan
- <sup>31</sup> APL
- <sup>32</sup> INAF, Bologna, Italy
- <sup>33</sup> University of Wisconsin-Madison
- <sup>34</sup> MIT
- <sup>35</sup> Yale University
- <sup>36</sup> University of Maryland, College Park
- <sup>37</sup> University of Maryland, Baltimore County
- <sup>38</sup> ESA
- <sup>39</sup> University of Colorado, Boulder
- <sup>40</sup> Universität Potsdam, Germany
- <sup>41</sup> MPIA, Heidelberg, Germany
- <sup>42</sup> Trinity University, Texas
- <sup>43</sup> Friedrich-Alexander Univ. Erlangen-Nürnberg, Germany
- <sup>44</sup> Saitama University, Japan
- <sup>45</sup> Leiden University, the Netherlands
- <sup>46</sup> University of Tokyo, Japan
- <sup>47</sup> Tel Aviv University, Israel
- <sup>48</sup> Pennsylvania State University
- <sup>49</sup> University of Washington

- <sup>50</sup> University of Chicago
- <sup>51</sup> Università degli Studi di Palermo, Italy
- <sup>52</sup> INAF, Palermo, Italy
- <sup>53</sup> Purdue University, Fort Wayne

[lem-observatory.org](http://lem-observatory.org)

## 1 SUMMARY

The Line Emission Mapper (*LEM*) is an X-ray Probe for the 2030s that will answer the outstanding questions of the Universe’s structure formation. It will also provide transformative new observing capabilities for every area of astrophysics, and to heliophysics and planetary physics as well. *LEM*’s main goal is a comprehensive look at the physics of galaxy formation, including stellar and black-hole feedback and flows of baryonic matter into and out of galaxies. These processes are best studied in X-rays; as emphasized by the 2020 Decadal Survey, emission-line mapping is the pressing need in this area. *LEM* will use a large microcalorimeter array/IFU (that builds on *Athena* XIFU technology developments), covering a  $30 \times 30'$  field with  $10''$  angular resolution, to map the soft X-ray line emission from objects that constitute galactic ecosystems. These include supernova remnants, star-forming regions, superbubbles, galactic outflows (such as the Fermi/eROSITA bubbles in the Milky Way and their analogs in other galaxies), the Circumgalactic Medium in the Milky Way and other galaxies, and the Intergalactic Medium at the outskirts and beyond the confines of galaxies and clusters. *LEM*’s 1–2 eV spectral resolution in the 0.2–2 keV band will make it possible to disentangle the faintest emission lines in those objects from the bright Milky Way foreground, providing groundbreaking measurements of the physics of these plasmas, from temperatures, densities, chemical composition to gas dynamics. While the mission is optimized to provide critical observations that will push our understanding of galaxy formation, *LEM* will provide transformative capability for all classes of astrophysical objects, from the Earth’s magnetosphere, planets and comets to the interstellar medium and X-ray binaries in nearby galaxies, AGN, and cooling gas in galaxy clusters. In addition to pointed observations, *LEM* will perform a shallow all-sky survey that will dramatically expand the discovery space.

## 2 MISSION CONCEPT

The Line Emission Mapper (*LEM*) is an X-ray Probe concept aimed at one of the fundamental unsolved problems of modern astrophysics — galaxy formation. Galaxies are governed by the competi-

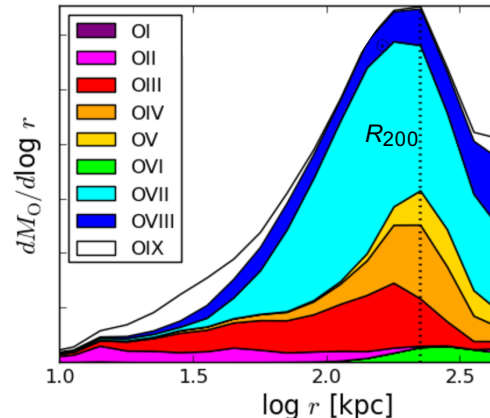


**Fig. 1** — Why soft X-rays? Predicted fraction of Oxygen ions in a CGM halo of a Milky-Way mass galaxy (simulations using EAGLE model<sup>16</sup>; dotted line is the virial radius; vertical scale is linear). Probing this circumgalactic gas is critical to understanding the physics of galaxies. The temperature of the halo is such that the dominant species over most of the halo is OVII, whose emission (along with that of OVIII) lies in the soft X-ray band — the energy of the Oxygen He $\alpha$  resonant line is 574 eV. The lower ionization species are observable in the UV, but modeling and extrapolation are required to deduce the properties of the CGM. An X-ray instrument will probe the bulk of the CGM directly, complementing the UV data on the cooler gas phases.

tion of gravity and the energetic “feedback” from the forming stars and black holes. Theoretical studies predict that key information on these processes is encoded in the tenuous Circumgalactic Medium (CGM) and even more rarefied Intergalactic Medium (IGM), which together contain most of the baryonic matter in the Universe<sup>3</sup>. Most of that matter has so far eluded detection, much less detailed study. The Astro2020 Decadal Survey has identified mapping CGM and IGM *in emission* as the key missing observing capability and a major “discovery area.” *LEM* is designed to provide this new capability in the soft X-ray band, where the dominant CGM and IGM ion species emit (Fig. 1). While the importance of studying these hidden baryons has been recognized for decades, only now has the technology arrived that makes it possible.

*LEM* is a single telescope that consists of an X-ray mirror with a large collecting area and moderate angular resolution, and a cryogenic microcalorime-



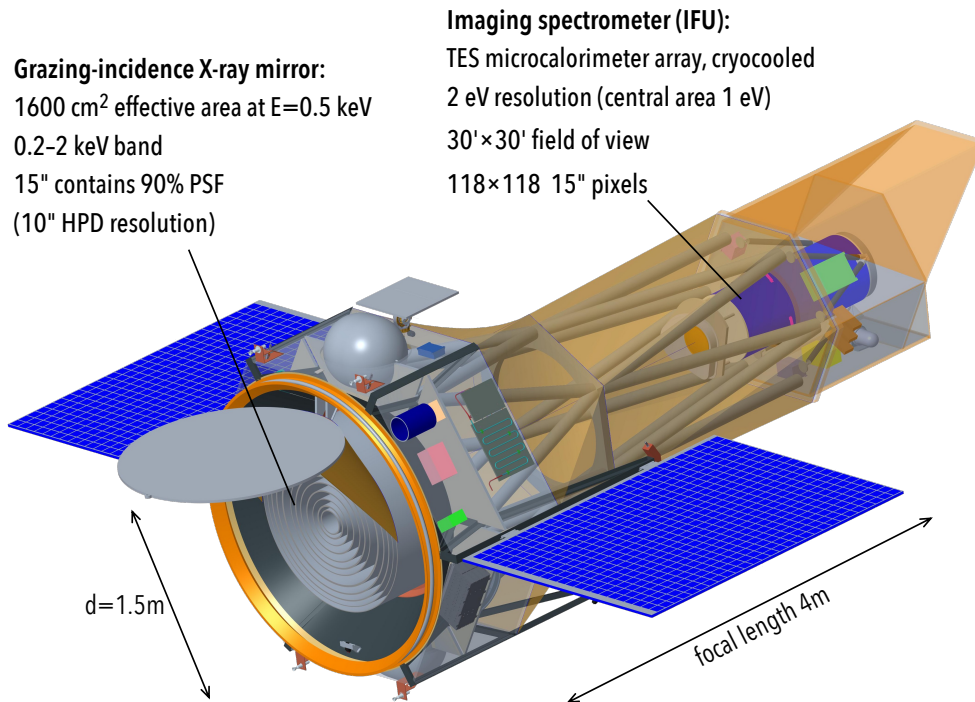


**Fig. 2** — *LEM* mission design (under development in collaboration with Lockheed Martin Corp.; a snapshot as of November 2022 is shown).

ter array (Fig. 2). Both are optimized for the 0.2–2 keV energy band, where the most abundant CGM/IGM ion species have multiple bright emission lines. Because the CGM and IGM are diffuse sources, mapping them requires a *nondispersive* imaging spectrometer, or an integral field unit (IFU) as they are known in other wavebands. (*Chandra* HETG and LETG, *XMM-Newton* RGS and the *ARCUS* concept are dispersive spectrometers whose full spectral resolution is available only for point sources.) Furthermore, as will be seen below, our own Milky Way places a bright screen in front of the very faint IGM and CGM around other galaxies. Removing this foreground requires eV-class spectral resolution. These two conditions require a microcalorimeter. Such imaging X-ray calorimeters have not been flown before, with the exception of the short-lived *Hitomi*, to be replaced in 2023 by *XRISM*. *LEM* will provide a leap beyond *XRISM*, and surpass in relevant capabilities other missions planned for the more distant future. Table 1 compares *LEM* to future X-ray microcalorimeters — namely, *XRISM* Resolve, *Athena* XIFU (to be launched in late 2030s) and *HUBS* (under study). The effective area and “grasp” as functions of en-

ergy for *LEM*, *XRISM* and *Athena* are compared in Fig. 3. We note that *Athena* is currently undergoing redefinition and as of this writing its final instrument parameters are unknown. The above comparisons are done with the pre-2022 *Athena* concept.

The *LEM* concept is being prepared for the NASA 2023 Astrophysics Probes call for proposals. If selected, *LEM* will be launched in 2032.

## 2.1 X-ray mirror

The grazing-incidence mirror will consist of many pairs (for two reflections) of thin monocrystalline silicon shells, coated with either Ir or Pt to provide X-ray reflectivity. The mirror’s 1.5m diameter and 4m focal length are selected to provide a large effective area at the energies of interest ( $E < 2$  keV) and a broad angular field of view, covering a Milky Way like galaxy at  $z = 0.01$  (40 Mpc), to fit within the detector of a feasible linear size. This choice of geometry means that the effective area at higher energies is low. The mirror is being developed at NASA GSFC. The angular resolution requirements imposed by the main science drivers is modest, 10" half-power diameter (HPD) or 15" square pixel enclosing 90% energy. A resolution of 2.8" HPD has

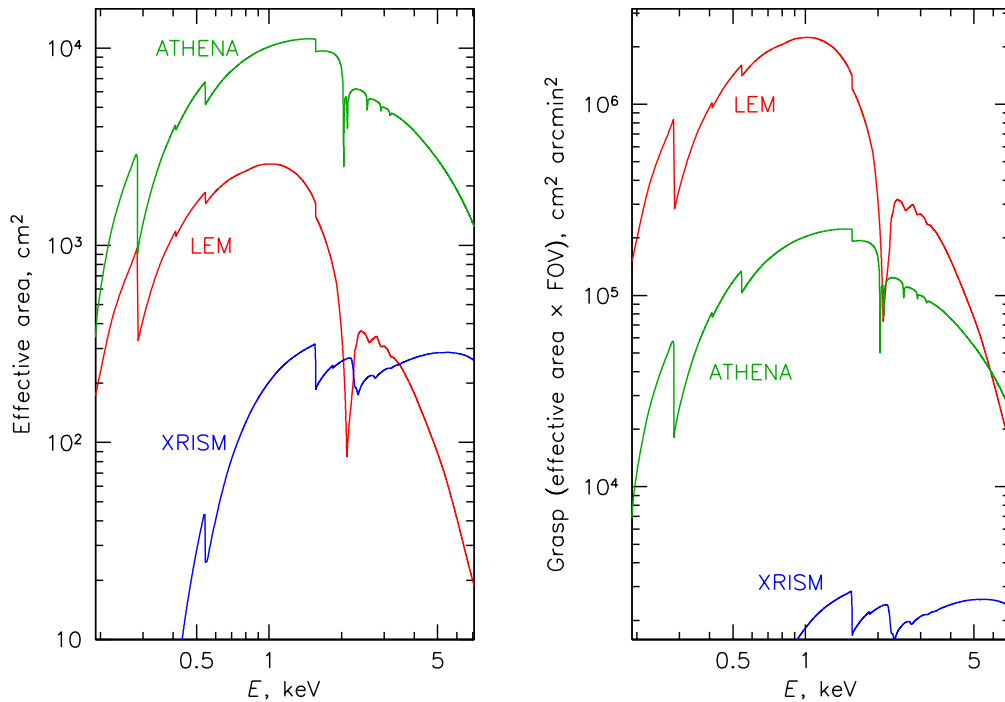


**Fig. 3** — *LEM* effective area and grasp — the product of the effective area and the field of view solid angle — compared to *XRISM* Resolve and *Athena* XIFU (prior to 2022 reformulation). Grasp is the quantity relevant for mapping faint extended objects with sizes comparable to or greater than the field of view (such as nearby galaxies, clusters, the IGM, or the Milky Way structures) — for such targets, the number of photons collected in a given exposure is directly proportional to grasp.

		LEM	XRISM Resolve	Athena XIFU*	HUBS
Energy band, keV		0.2–2	0.4–12	0.2–12	0.2–2
Effective area, cm <sup>2</sup>	0.5 keV	1600	50	6000	500
	6 keV	0	300	2000	0
Field of view		30′	3′	5′	60′
Grasp, 10 <sup>4</sup> cm <sup>2</sup> arcmin <sup>2</sup>	0.5 keV	140	0.05	12	180
Angular resolution		15″	75″	5″	60″
Spectral resolution		1 eV (central 7′), 2 eV (rest of FOV)	7 eV	2.5 eV	2 eV
Detector size, pixels (equiv. square)		118×118	6×6	50×50	60×60

**Table 1** — *LEM* compared with the requirements for the future X-ray nondispersive spectrometers onboard *XRISM* (JAXA/NASA), *Athena* (ESA/NASA) and *HUBS* (Chinese Space Agency). For *XRISM*, based on *Hitomi*, the actual spectral resolution is expected to be 5 eV. The main advantages of *LEM* are its large grasp and high spectral resolution. \*For *Athena*, pre-reformulation requirements are listed.

already been demonstrated in the lab for a small subset of the mirror (Fig. 4). The mirror is designed to have a constant PSF and insignificant vignetting across the  $30'$  field of view.

## 2.2 Detector

The *LEM* detector is a cryocooled array of Transition-Edge Sensor (TES) microcalorimeters. It will be built at NASA GSFC using the technology developed for *Athena* XIFU and the *Lynx* concept by the same team<sup>9,11</sup>. The array will consist of 13,806 absorber pixels (equivalent of  $118 \times 118$  square) with a  $290 \mu\text{m}$  pitch, in hexagonal arrangement. For a 4m focal length, it will cover a solid angle equal to a  $29.4'$  square.

The inner 1062 absorber pixels (a  $7' \times 7'$  square array) will each be connected to a single TES and provide an energy resolution of 1 eV (FWHM). The rest of the array will consist of “hydras,” where  $2 \times 2$  absorber pixels are connected to a single TES, which will determine which absorber was hit with a photon based on the different time constants for the different absorbers<sup>23</sup>. These pixels will provide a resolution of 2 eV (FWHM) for  $E < 2 \text{ keV}$ . The absorber thickness will be optimized for the low X-ray

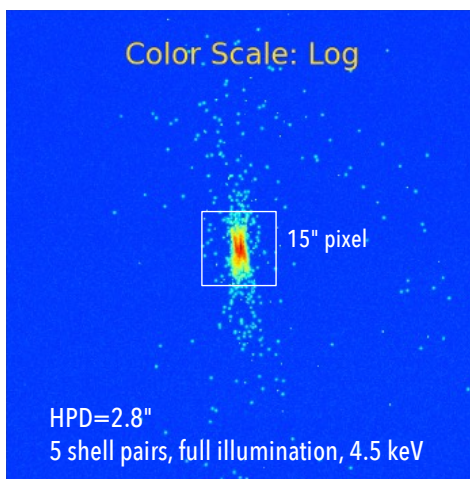


**Fig. 4** — Point Spread Function measurement for a subset of the mirror consisting of 5 pairs of reflective shells. The image is elongated because it comes from an incomplete mirror. A  $2.8''$  HPD is achieved for this subset; the requirement is  $10''$  HPD (or, equivalently, for 90% of the photons to fall in the  $15''$  detector pixel) for the whole *LEM* mirror that will combine approximately 3500 shell pairs.

energies and the sensor will take advantage of the narrow energy band of the mirror. Figure 5 shows the measured line response for a prototype *LEM* array<sup>24</sup>, which already nearly meets our requirements both for the single pixels and the hydras. The position discrimination within the hydra has also been demonstrated at least for  $E > 300 \text{ eV}$ .<sup>24</sup>

*LEM* will use the IR and optical blocking filters developed for *Athena* XIFU, scaled up in size for a wider viewing cone of the *LEM* mirror.

The calorimeter array is cooled to the 35 – 50 mK operating temperature by the Adiabatic Demagnetization Refrigerators built at NASA GSFC and the cryocooler built by Lockheed Martin.

A modulated X-ray source will operate in orbit and illuminate the array with a 1.5 keV Al  $K\alpha$  near-monochromatic line for continuous calibration of the energy response. The resulting accuracy on the pixel energy gain, 0.25 eV at 1.5 keV (and proportionally lower at lower energies), corresponds to a 50 km/s accuracy ( $1\sigma$ ) on the relative velocity measurements using the Doppler shift.

## 2.3 Spacecraft and orbit

The spacecraft will be built by Lockheed Martin Corp. The main mode of operations will be long pointed observations. *LEM* will also be able to slew to perform efficient scans of large areas of the sky — such as the whole sky (§3.2). While *LEM* is not a time-domain mission and not required to have a fast response capability, it will be able to respond to the highest-profile events on a several-day timescale from first notice to pointing — similar to *Chandra*. The area of the sky accessible at any particular moment will be approximately half the sky; this fraction is currently under study.

The orbit for *LEM* is currently under study. The Sun-Earth Lagrange points L1 and L2 would provide a stable thermal environment for the microcalorimeter and the high observing efficiency to take full advantage of the 5 yr mission minimum lifetime. A possibility to extend the field of regard to include observations of the Earth’s magnetosphere from the L1 orbit is being considered.

## 3 SCIENCE DRIVERS

Below is a brief description of the science investigations that will be enabled by *LEM*. They will be

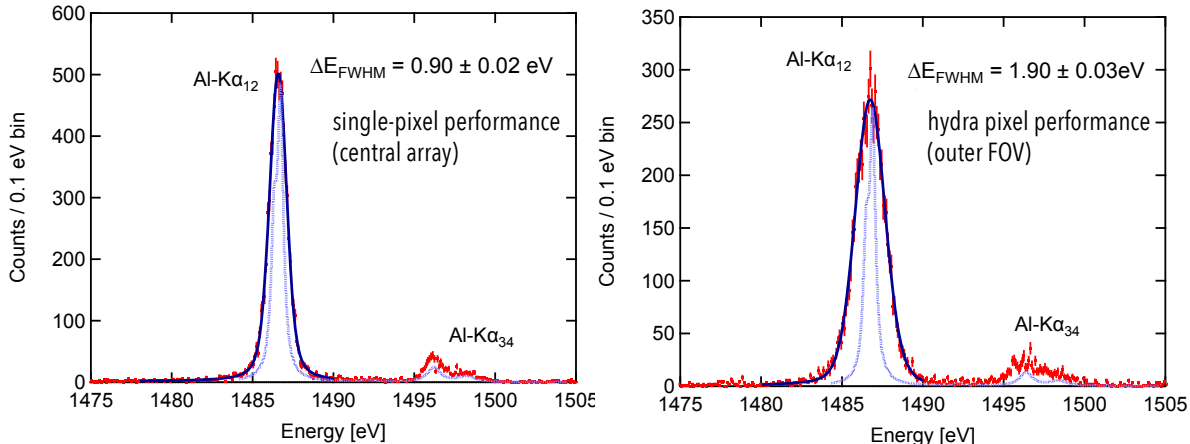


**Fig. 5** — Spectral resolution for a prototype *LEM* detector array<sup>24</sup>, measured for the single-absorber pixels (the central array) and the 4-pixel hydras (the rest of the detector). The measurements were performed at  $E = 1.5$  keV. The blue dotted line is the intrinsic Al line profile (arbitrary normalization) and the black line is the model that includes detector broadening. The performance already nearly meets the *LEM* requirements.

presented in more detail in several forthcoming papers.

### 3.1 Physics of galaxy formation

Galaxies form from the collapse of primordial matter density fluctuations under the effect of gravity, which is counteracted by feedback from stars and the central supermassive black holes that pushes the gas out of the galaxy. The result is a circulation of gas and metals (synthesized by stars and supernovae in galaxies) into and out of galaxies — a galactic ecosystem. Understanding this ecosystem is key to understanding galaxy formation. Quoting Astro2020, “the key missing link in unveiling the physics driving galaxy growth is to measure the properties of the diffuse gas within, surrounding, and between galaxies,” and these three locations constitute the main *LEM* science drivers.

**CGM.** At the mass scale of the Milky Way, the observable galaxy properties exhibit a dramatic change — from star-forming disks thought to be fed by cold gas streams, to passive ellipticals surrounded by hot hydrostatic gas. Apparently, this reflects the shift in the balance of the various galaxy-shaping physical processes. Galaxies around this mass should thus offer a particularly sensitive probe of those processes. Indeed, cosmological simulations of the MW-mass galaxies that include different physics make strikingly different predictions for the X-ray properties of the outer regions of the circumgalactic halos (Fig. 6). At present, these predictions

are entirely unconstrained by observations, and detecting and measuring this X-ray signal can tell us

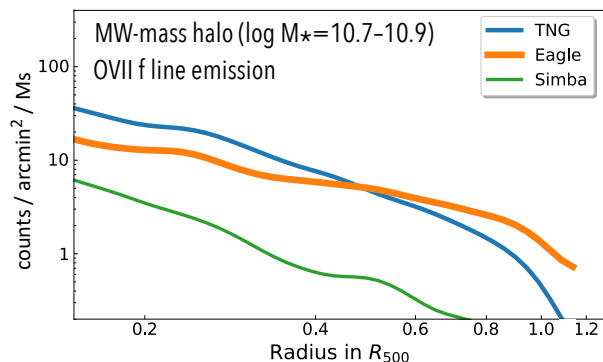


**Fig. 6** — Predicted brightness profiles of the OVII emission for Milky Way mass galaxies from three cosmological simulations (TNG<sup>13</sup>, EAGLE<sup>22.5</sup>, Simba<sup>6</sup>). OVII is abundant at  $T = (0.3 - 2) \times 10^6$  K that is characteristic of CGM. Each curve is a median profile for 50 simulated galaxies. The expected *LEM* counts are shown for a 2 eV wide interval centered on the forbidden line of the OVII triplet at  $z = 0.01$ .  $R_{200} \simeq 1.5R_{500}$ . These numerical models include different physical prescriptions for feedback, and the resulting predicted X-ray brightness at large radii differs by over an order of magnitude. The CGM extent and spatial structure are sensitive diagnostics of the feedback physics; detecting and mapping this emission will strongly constrain the physical processes shaping the galaxies.

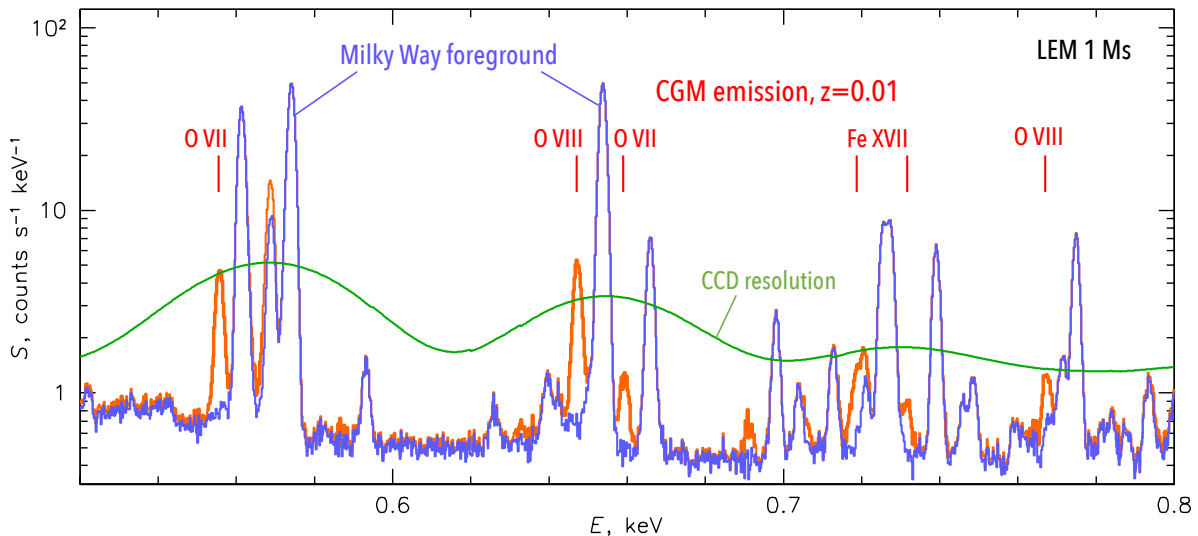


**Fig. 7** — Simulated *LEM* spectrum of the CGM of a galaxy twice as massive as the Milky Way (from TNG simulations<sup>13</sup>), at  $z = 0.01$  or 40 Mpc, for a 1 Ms exposure and the 2 eV resolution of the full detector. Blue line shows the spectrum of the foreground, red line includes the CGM signal. The spectrum is extracted from a broad annulus between  $0.25 - 0.75 R_{500}$ . Point sources detected with the *LEM* angular resolution are excluded. Because the Milky Way emits in the same spectral lines but is over an order of magnitude brighter, it is impossible to disentangle the two with the present CCD instruments such as *Chandra* and *XMM-Newton* (green line). A nondispersive spectrometer with 2 eV resolution allows the study of the faint CGM for galaxies at  $z \gtrsim 0.01$ , where they can also be well-resolved spatially.

which physical processes shape the CGM.

*LEM* will be able to map the CGM (defined here as the gaseous halo within the galaxy virial radius  $R_{200}$ ) in the emission lines of the dominant ion species, OVII, OVIII and FeXVII. The high spectral resolution will allow us to disentangle the faint signal from the CGM of external galaxies from the overpowering Milky Way foreground using the galaxy’s redshift. Because the Milky Way itself has a CGM halo that emits in the same atomic transitions — and we are immersed in its bright central region and see that emission across the sky — the ability to separate the redshifted extragalactic signal by energy is a critical advantage of *LEM*, as illustrated in Fig. 7. The current X-ray CCD detectors lack spectral resolution for this approach.

For the Milky Way mass halos, *LEM* will be able to map the CGM emission for individual galaxies (as opposed to stacking the radial profiles of many galaxies) in the brightest emission lines out to  $R_{500}$  and beyond, and derive the distribution of gas temperature, density, pressure and elemental abundances out to a large fraction of  $R_{500}$ . The maps are expected to reveal a wealth of spatial structure,

possibly including the extragalactic analogs of our own Milky Way’s Fermi bubbles (Fig. 8) — if black hole / AGN feedback is as important as theory predicts. Such measurements are only possible because the Milky Way foreground can be separated using the redshift of the signal. The minimum redshift for such separation for the 2 eV detector resolution is  $\sim 0.01$  (Fig. 7); at this redshift, the  $R_{500}$  for a Milky Way mass galaxy fills the *LEM* FOV and the whole galaxy can be mapped in one deep pointing. The *LEM* angular resolution will allow efficient spatial masking of the background point sources and resolving the interesting linear scales in the halo (e.g., shocks around the Fermi bubbles). A typical CGM halo is optically thin for the emission lines of interest over most of its volume except for the very central regions, where the optical depth for the OVII resonant line becomes significant. *LEM* will easily resolve the components of the OVII He $\alpha$  triplet (where the resonant line is affected by scattering while other components are not), which will enable interesting physical diagnostics of the gas.

Using the high-resolution (1 eV) central array, *LEM* will be able to simultaneously map the veloci-



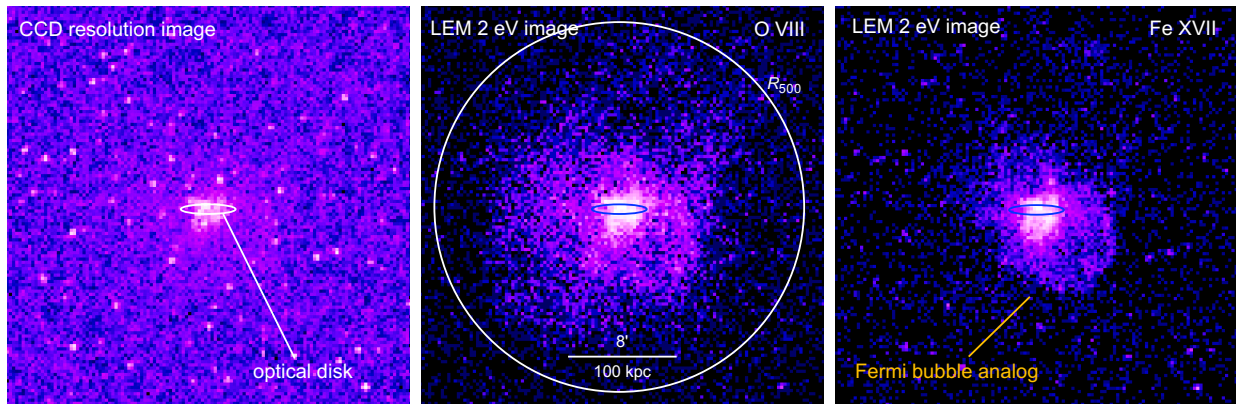


**Fig. 8** — Simulated Milky Way-like galaxy at  $z = 0.01$  (TNG50<sup>18,19,14</sup> of the IllustrisTNG simulation suite). Panels are  $30'$  with  $15''$  pixels (*LEM* field of view and angular resolution). The ellipse shows the size of the optical disk, seen edge-on. *Left*: Soft X-ray image with a CCD-like ( $70$  eV) spectral resolution centered at the OVIII line, including the Milky Way foreground and CXB (the brightest sources accounting for half of CXB flux have been spatially removed). The bright foreground makes it impossible to detect extended CGM emission. *Middle, Right*: *LEM* 1 Ms images of the same galaxy, but in  $2$  eV wide bins (the *LEM* spectral resolution) centered on the OVIII and FeXVII CGM emission lines. The MW foreground is almost completely resolved away, taking advantage of the galaxy’s known redshift; the use of the narrow bin also removes most of the residual power-law CXB flux. *LEM* unveils the rich spatial structure of the line-emitting CGM halo — including the analog of the Fermi/eROSITA bubbles produced by the central SMBH. Mapping different emission lines provides a measurement of the plasma temperature.

ties in the brighter central regions of the galactic halos. It will detect gas bulk velocities and velocity dispersion predicted for the particularly energetic modes of feedback.

**IGM.** An even more challenging observing target is the IGM, which we define as the diffuse matter outside  $R_{200}$  of any galactic or cluster halos. The warm-hot phase of it ( $> 10^5$  K) is known as WHIM. It is the ultimate repository of everything expelled from the galaxies over their lifetime, and its metal content thus encodes the history of the feedback processes in the Universe. The IGM regions immediately surrounding massive hot galaxy clusters, where the gas temperature is still above  $10^7$  are accessible for sensitive low-background CCD instruments, which could use the emission at  $E > 1$  keV. However, most of the IGM has lower temperatures, and its emission will be flooded by the bright Milky Way. *LEM* will be able to detect the brightest emission lines from the dense regions of the Cosmic Web filaments that connect galaxy clusters, at distances  $2R_{200}$  from the clusters and beyond.

We will use optical galaxy redshift surveys to select such filaments at an optimal redshift ( $z =$

$0.07 - 0.08$ ) to be able to see the most promising IGM emission lines through the Milky Way line forest (Fig. 9) and survey these regions with multiple deep pointings. This is where the large grasp is critically important, as the number of photons collected from a very extended source is directly proportional to it — and the IGM is extremely faint. While we will not be able to detect the *continuum* emission from the IGM (it is too far below the background), we will detect the faint emission lines of OVII, OVIII and FeXVII (if, that is, the IGM is indeed enriched, as the current theory predicts), and compare the brightness in these lines as a function of the galaxy number density with cosmological simulations, in order to determine when the enrichment of the IGM by galactic ejecta has occurred and what physical processes were responsible.

*LEM*’s large grasp and good angular resolution will allow us to detect the IGM *in absorption* in the cumulative spectra of the CXB sources in the same fields where we will search for the IGM emission. A comparison of emission and absorption for the same filament will allow us to derive the physical properties of the filament gas.

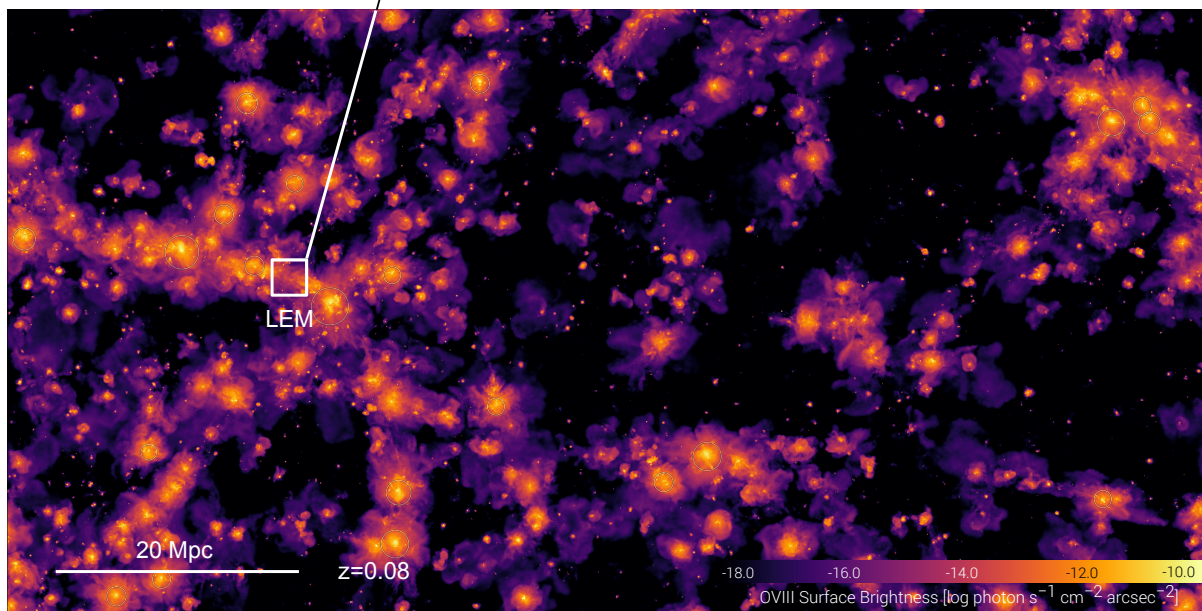
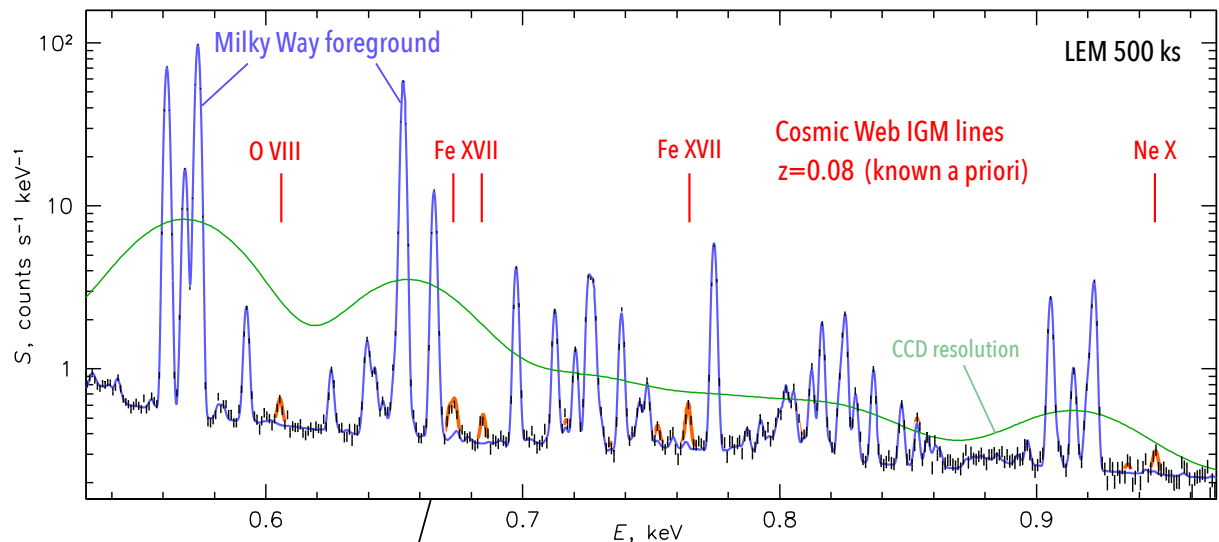


**Fig. 9**— Simulated *LEM* spectrum of the Intergalactic Medium (IGM) in the Cosmic Web. Owing to its high spectral resolution and large grasp, *LEM* will be able to detect emission from metals in the denser regions of the Cosmic Web filaments, outside the confines of galaxies (and their CGM halos) and galaxy clusters. It is a diagnostic of galaxy formation processes at early epochs. Filaments will be selected from galaxy surveys and the redshift of the IGM will be known, i.e., it is not a blind search for emission lines. The image shows OVIII emission in cosmological simulations (TNG100<sup>12</sup>). The sample spectrum corresponds to a typical bright region of an IGM filament near a massive cluster (at a distance  $r \sim 2R_{200}$  from the cluster), excluding halos of all galaxies and clusters. The eV spectral resolution is essential for separating the faint IGM lines (highlighted by red) from the much brighter Milky Way foreground (cf. the green line that shows the same spectrum at CCD resolution).

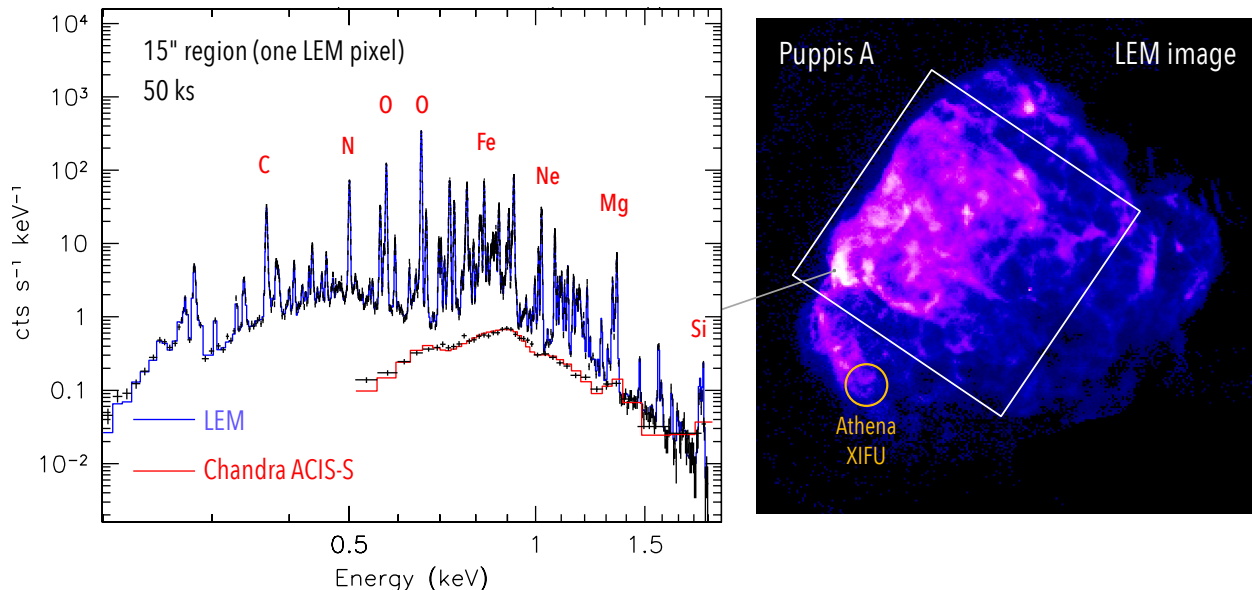


**Fig. 10** — *Left*: Sample spectrum from one pixel in the *LEM* calorimeter from a 50 ks exposure of the Puppis A supernova remnant. *Right*: *LEM* image of Puppis A. The white square shows one *LEM* FOV and the circle shows the *Athena* XIFU FOV. *LEM* will map such large SNRs very efficiently, which is especially valuable for old, large Galactic SNRs. Each *LEM* pixel will provide an extremely line-rich spectrum, resolving multiple lines for each ion, allowing us to map chemical composition, diagnose nonequilibrium conditions in the plasma and measure velocities of ejecta. A CCD spectrum (*Chandra* ACIS) is shown for comparison; all spectral features are blended. A dispersive spectrometer (gratings) provides very limited spectral resolution for such extended sources because of spatial blending.

The line emission from the low-density IGM can be significantly enhanced (in the resonant transitions only), compared to intrinsic thermal emission, by resonant scattering of the CXB photons, if the CXB point sources are excised from the image<sup>8</sup>. This improves the detectability of the IGM emission. This also applies to the outer regions of the CGM, with a significant additional enhancement from the resonant scattering of the photons from the galaxy’s own bright central region. This will extend the radius at which the CGM could be detected by *LEM*. Of course, interpretation of the detected signal will require modeling of the scattered contribution; *LEM* will be well equipped for such spectral diagnostics because it will resolve the resonant and forbidden transitions for the relevant ions.

**Abundances in the ICM.** *LEM* will address the cumulative effect of the galactic feedback from another angle. The ratios of the various elements in the ICM in the outskirts of galaxy clusters, as well as the total metal content of the ICM and the spatial distribution of metals in the ICM, depend on the prevalent star populations and types of supernovae

that generated those metals, when it happened, and how the metals mixed into the intergalactic gas<sup>10</sup>. *LEM* will map the abundances and abundance ratios for O and Fe, but also for a number of less-abundant elements that can be used as sensitive diagnostics for the sources of chemical enrichment. *LEM*’s large grasp and good angular resolution will allow us to efficiently and completely map the abundances of all the interesting elements in nearby groups and clusters in the interesting radial range  $0.5R_{500} - R_{200}$ .

**Velocities of the ICM.** *LEM* will efficiently and completely map the gas velocities and velocity dispersions in nearby clusters and groups, relaxed and dynamic, out to  $R_{200}$  (using mostly the Fe-L lines). It will determine where the clusters are hydrostatic and where the contribution of turbulence and gas bulk motions into the total energy budget becomes important. This information is key for our understanding of the physics of the large scale structure and cluster formation.

**Stellar feedback.** *LEM* will study the gas inside the Milky Way that is part of the galactic ecosystem. It will map the chemical composition



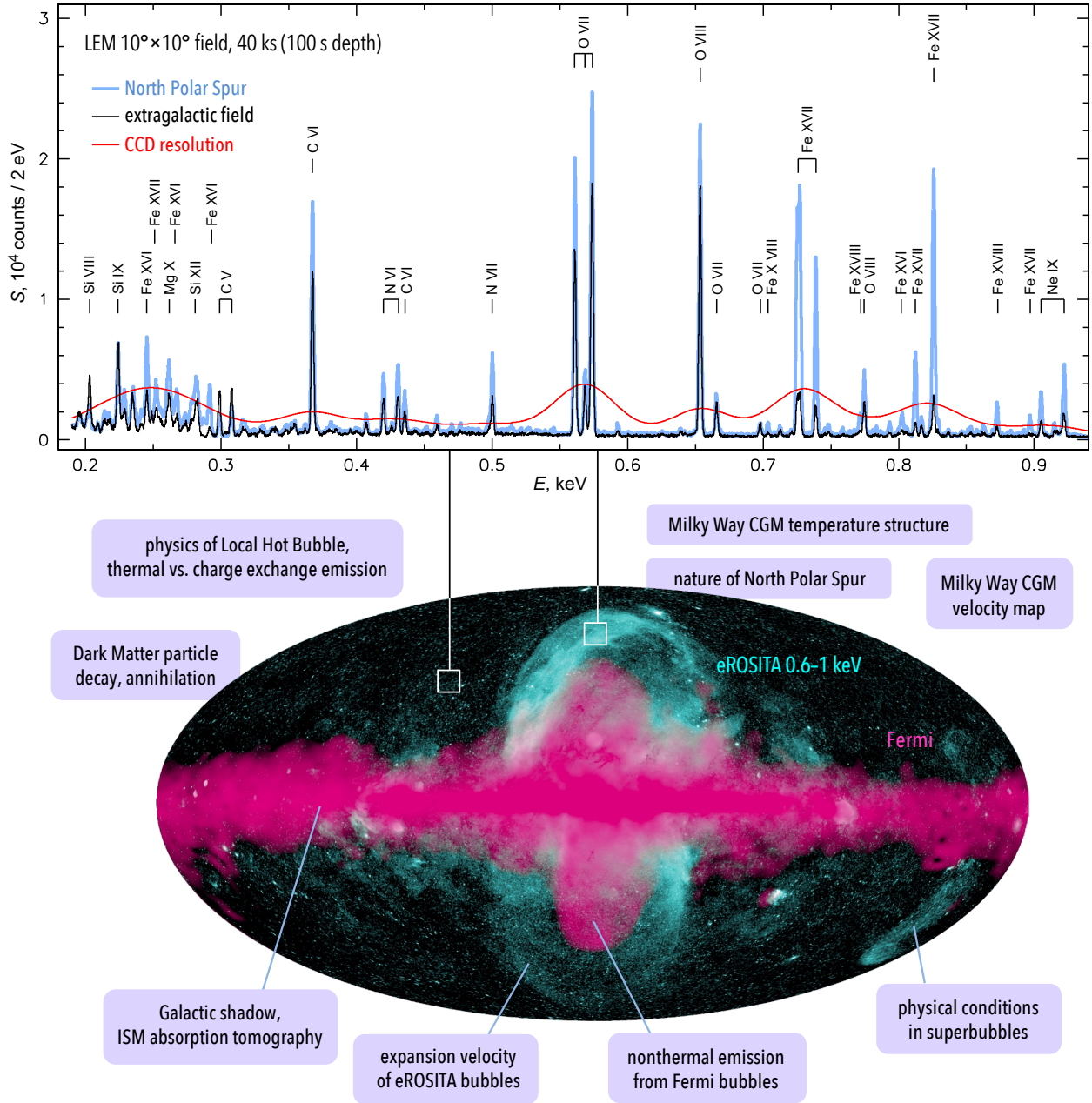


**Fig. 11** — *LEM* shallow all-sky survey. The all-sky map<sup>20</sup> in Galactic coordinates overlays soft X-ray emission from *SRG/eROSITA* (cyan) and  $\gamma$ -ray emission from *Fermi* (magenta). *Top*: Example simulated spectra for  $10^\circ \times 10^\circ$  regions (marked by squares) and 100s depth are shown for an average high-latitude region outside of any bright features (“extragalactic field”), and another for the North Polar Spur; the CXB is included. Purely thermal CIE plasma models are assumed. Red curve shows the NPS spectrum at CCD resolution (e.g., *eROSITA*). *LEM* will resolve the forest of lines and gain access to line diagnostics for temperature, nonequilibrium and charge exchange processes. The survey will allow us to map the temperature structure and velocities of the Milky Way inner CGM on few-degree scales — including the expansion of the *eROSITA*/*Fermi* bubbles, believed to be produced by the central SMBH or star-forming regions. Numerous other investigations, some of which are labeled in the figure, will become possible.



and velocities of ejecta in well-resolved supernova remnants Fig. 10). It will also map the physical conditions in the Milky Way and Local Group superbubbles — regions where stellar winds from many massive stars and the supernovae combine and form large cavities in the ISM filled with hot plasma. If superbubbles break, the hot plasma can escape from the galactic disk, forming galactic outflows or fountains and flowing into the CGM. This is the mechanism by which the stellar feedback in galaxies operates. Mapping the X-ray line emission will offer diagnostics of gas out of collisional ionization equilibrium (rapidly heating/cooling) and separating thermal emission from the charge exchange emission that arises from the mixing of cold and hot gas phases. With its large grasp, *LEM* will be able to efficiently map very extended structures as Orion-Eridanus and other nearby superbubbles.

### 3.2 All-Sky Survey

As described above, the IGM and the CGM of external galaxies are observed through the forest of bright Milky Way emission lines. It will be helpful to find areas in the sky where this foreground is less bright, at least in certain problematic lines such as FeXVII and FeXVIII. (This is similar to *Hubble* peering into the Lockman Hole to observe high- $z$  galaxies.) The *eROSITA* and *HaloSat* sky surveys will be helpful, but lack spectral resolution to detect faint emission lines. *LEM* has sufficient grasp to perform its own shallow all-sky survey in a relatively modest total exposure — e.g., an all-sky coverage with a useful 10s depth will require 1.6 Ms. We envision performing such shallow pathfinder survey very early in the mission to identify areas in the sky best suited for deep CGM/IGM exposures and for other interesting studies, and add up to 10 times more depth over the mission lifetime.

In addition to the above technical purpose, the first-ever all-sky survey with an imaging calorimeter will open **enormous discovery space**. With *LEM*'s large effective area, even a shallow depth will be sufficient for groundbreaking studies. The statistical quality and richness of the spectra for typical low-brightness and high-brightness regions of the sky for the eventual full depth are illustrated in Fig. 11. The figure also lists examples of investigations using all-sky or partial-sky data that we can envision at present.

Some important aspects of the **feedback processes** in Milky-Way mass galaxies would be best viewed from inside the Milky Way. *LEM* will map the velocities of the inner regions of the Milky Way CGM, and in particular, the expansion of the Fermi/eROSITA bubbles, believed to be evidence of feedback from either the SMBH or star-forming regions in the Galactic Center. It will map the temperature structure of the inner CGM across the sky and along the line of sight using lines of the various ion species — something only a calorimeter can do, in the presence of multiple temperature components and solar wind charge exchange on each line of sight. The MW observations will complement the studies of CGM in other galaxies (§3.1), where *LEM* will map the outer halos but have limited insight into the interface between the disk and the halo, where the exchange of mass and metals with the outer CGM takes place.

The emission of the lower MW halo (thought to be formed from the exhaust of Galactic chimneys) can be separated from the emission of the Galactic disk ISM by observing a dense absorbing extraplanar cloud, and determining the spectra of the foreground and background to the cloud. *LEM*'s large FOV and high spectral resolution will allow the first definitive separation of the disk and halo spectra for individual plasma diagnostics.

*LEM*'s sensitivity and spectral resolution at low energies will let us unambiguously separate the heliospheric solar wind charge exchange (SWCX) line emission from thermal emission of the Local Hot Bubble (LHB) and the Galactic halo. This will let us explore the physics of the LHB. The North Polar Spur is another enigmatic structure in the Milky Way sky, possibly projected onto the northern Fermi bubble (Fig. 11); its spectrum is known (at CCD resolution) to be very different from the rest of the sky above the Galactic plane. A survey with *LEM* will provide the plasma temperature and velocity map for this feature, as well as any possible contribution from the charge exchange mechanism, and may explain its nature.

The Fermi bubbles (as distinct from the eROSITA bubbles that surround them, Fig. 11) contain cosmic ray electrons that generate the synchrotron “microwave haze” observed by *WMAP* and *Planck* and the inverse Compton  $\gamma$ -ray emission discovered by *Fermi*<sup>1</sup>. The synchrotron radiation gen-

erated by the highest-energy end of this population may be detectable in the soft X-ray band covered by *LEM*. *LEM* is a very sensitive instrument for detecting faint *continuum* emission at  $E < 1$  keV, because it can resolve away the emission lines that dominate the soft X-ray sky. *LEM* will have the requisite grasp to map the entire Fermi bubbles as part of the all-sky survey and yield constraints on the X-ray synchrotron emission from the southern Fermi bubble. *LEM* upper limits — or a positive detection — will provide insights into the energetics of the Fermi bubbles.

### 3.3 Observatory science

In addition to the main science drivers described above (which will be addressed during the 30% of the mission observing time allocated to the science team), *LEM* will transform all areas of X-ray astrophysics. It is useful to think of *LEM* as an *XMM-Newton* with a calorimeter — its imaging capabilities (FOV, angular resolution, effective area) are similar in the  $E < 2$  keV band to EPIC’s, while its spectral resolution is 50 times better. Many studies will be serendipitous to the long CGM and IGM exposures, while others will be proposed by general observers (GO) for the remaining 70% of the observing time. Many of them will need only modest exposures. An incomplete sample of possible novel short investigations is given below.

**Cooling, AGN feedback, gas mixing** in cool cores of galaxy clusters. Where is the coolest gas in the Perseus cluster core and how cool does it get? *LEM* will use its 1 eV resolution in the central array to derive the temperature distribution for the cooling gas. It will also map the charge exchange emission that may come from the interface between the hot ICM and the molecular gas nebula. If such emission is detected and spatially correlated with the cold nebula (for which at least a *LEM*-like angular resolution is required), it would provide invaluable insight into the process of gas mixing — a critical piece of the puzzle of the energy balance in the cluster cool cores.

**Power spectrum of turbulence** in cool galaxy clusters and groups using the velocity structure function. Because of its large grasp, *LEM* will be able to cover the entire cluster in a short exposure. The full spatial coverage greatly increases the accuracy of the structure function and the power spec-

trum measurement.<sup>26</sup> A power spectrum of turbulence will provide the measure of the energy flux from the cluster mergers down the turbulent cascade to the dissipation scale.

**Protoclusters at high  $z$ .** Deep exposures toward IGM and CGM fields will return significant numbers of serendipitous distant galaxy clusters, for which *LEM* will be able to determine the redshift using its own X-ray spectra. Dedicated surveys can be also devised. *LEM* will derive chemical abundances for high- $z$  clusters and constrain the cosmological enrichment history.

**High- $z$  AGN.** Every *LEM* deep field will have multiple AGN at  $z > 2.5$  with a detectable Fe  $K\alpha$  line. *LEM* will measure the profiles of these lines to study broad-line region clouds and accretion disk reflection. It will study heavily obscured AGN and expand significantly upon the AGN science derived from current *Chandra* and *XMM-Newton* deep fields.

**AGN outflows and feedback.** With its superior energy resolution, *LEM* will be able to precisely map fluorescent and photoionization lines and decouple AGN signatures in emission and absorption from ionization by stellar sources to understand the role that AGN outflows and feedback play in galaxy evolution.

**Hot ISM and X-ray binaries in nearby galaxies.** In face-on spirals, *LEM* will map the ISM dominated by emission lines and isolate the X-ray binaries (XRB) spatially and using their time variability. In nearby spirals such as M33 (Fig. 12), *LEM* will be able to study XRB populations and star-forming regions that are generally not detected in the Galaxy due to obscuration. We will be able to apply plasma diagnostics to determine whether the gas in and around star-forming regions is in CIE, or whether it has lost a significant amount of energy in expansion, while remaining in a strongly overionized state. This determination will be pivotal for understanding the formation of ISM superbubbles.

In accreting stellar-mass black hole systems, relativistically-broadened O-K and Fe-L lines are fluoresced off the surface of the accretion disk. These features can be used to constrain the accretion disk inner radius and/or black hole spin.

**Jellyfish galaxies.** *LEM* will map the process of ram-pressure stripping of galaxies traveling through

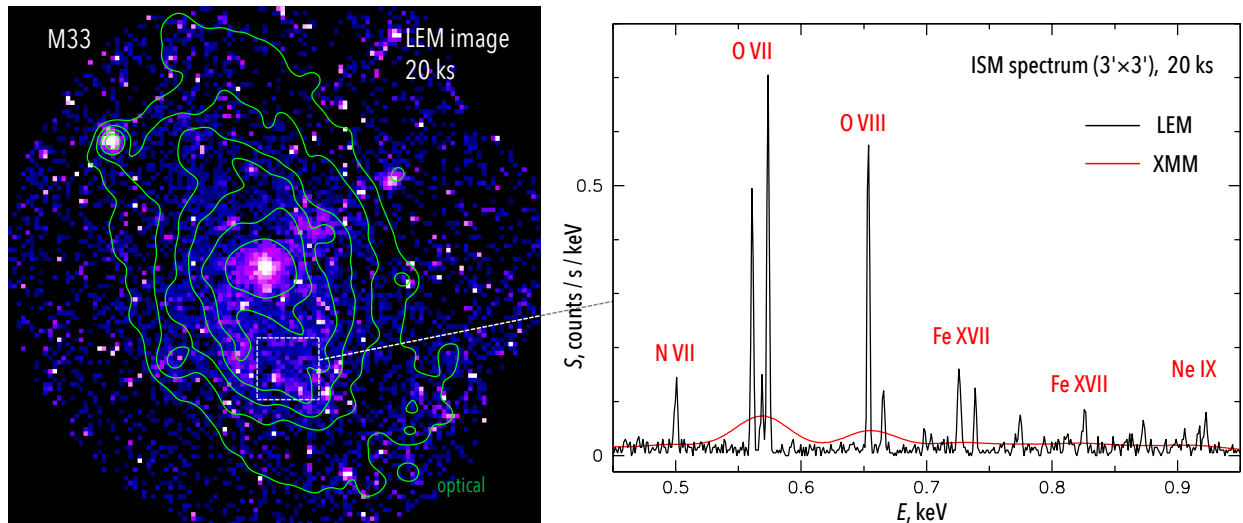


**Fig. 12**— *LEM* will be able to spatially separate and perform spectroscopy of the ISM and the X-ray binaries in nearby spiral galaxies, such as M33. A simulated 20 ks *LEM* image (based on the existing *XMM-Newton* observation) and a sample ISM spectrum are shown. *LEM* will detect many binaries and probe their variability. It will also produce detailed maps of the line-dominated ISM emission. For such nearby galaxies, the Milky Way foreground cannot be separated using the redshift, but its contamination for most ISM lines is under 10%. In each observation, *LEM* will provide the same amount of imaging information as *XMM-Newton*, but 20–30 times more spectral information.

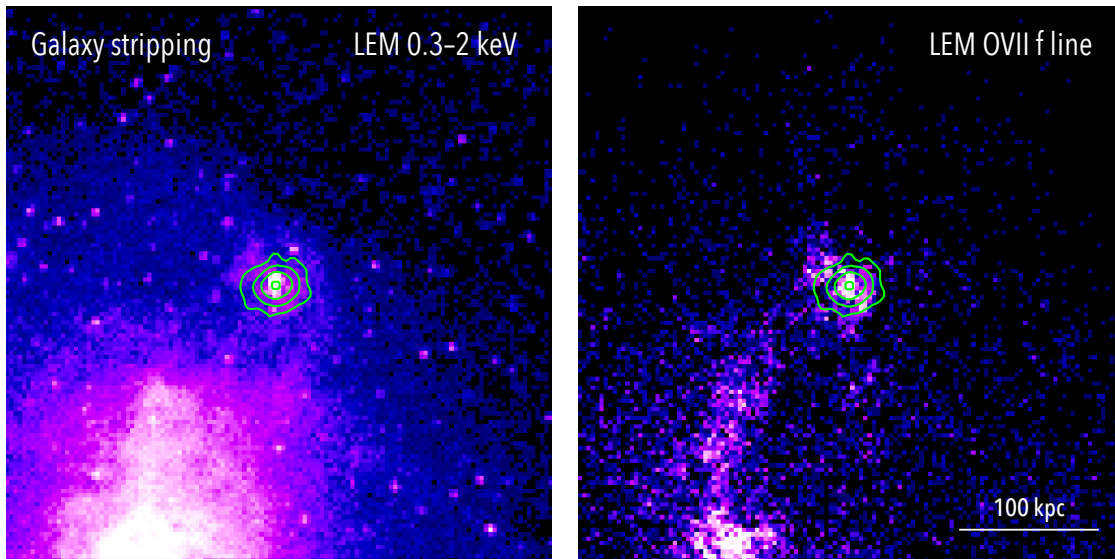
the gas in groups, clusters and the Cosmic Web filaments, and of galaxies undergoing collisions with other galaxies. This is an important mechanism by which the ICM and IGM are enriched by metals. *LEM* will be particularly well-equipped to detect the stripped gas and study its mixing with the ICM — a process that strongly depends on plasma physics and such properties as plasma viscosity, thermal conduction and the structure of its magnetic fields.

Figure 13 illustrates how *LEM* will use its energy resolution to separate the cool stripped gas, whose emission is dominated by certain lines, from the hotter ICM, revealing the morphology of the stripped tail, which strongly depends on plasma properties<sup>21</sup>. Furthermore, as stripping can bring neutral gas from the galaxy in direct contact with the hot ICM, one can in principle expect the charge exchange emission from their interface, with its tell-tale line signatures in the *LEM* spectra. This is a completely unexplored area that holds great promise for probing the ICM plasma physics. *LEM* will also study the effect of galaxy collisions and ram pressure stripping on ISM and star formation.

**Shocks in outskirts of massive galaxies.** As noted above (§3.1), the emission from the outer

regions of the CGM of massive galaxies may be enhanced by resonant scattering of the CXB photons<sup>8</sup> and of the photons from the galaxy’s own bright central emission. This “illumination” in the resonant OVII line may help *LEM* detect and map the outer reaches of the galactic halos, where OVII should be abundant but the intrinsic thermal emission is too faint. It is at those virial regions that we expect to find shock fronts from galaxy/galaxy mergers and matter infall. Recently, a radio phenomenon was discovered that may be caused by those shocks (“odd radio circles,” or ORCs, around massive galaxies at several hundred kpc from their centers<sup>15</sup>). *LEM* is well-equipped for detecting such shock features via their associated density jumps in thermal plasma, highlighted by the resonantly scattered light. This will uncover an additional piece of the galaxy formation puzzle. Such measurements will have to be done at  $z > 0.035$  in order to move the OVII resonant line from behind the MW OVII triplet.

**Light echo on giant molecular clouds** in the Galactic Center. The SMBH in the center of our Galaxy is quiescent at present, but may have been more active in past several hundred years. The light



**Fig. 13** — *LEM* will map the process of galaxy stripping and mixing of the stripped gas in detail. A 100 ks *LEM* exposure of interacting galaxies at  $z = 0.01$  (TNG100 simulations<sup>25</sup>) — an  $M_{\text{tot}} = 2 \times 10^{11} M_{\odot}$  galaxy (at the panel center, with contours showing optical light) after the passage through a group-mass halo (at the lower edge of the panels). The CXB is included, except for its brightest point sources, which are removed. *Right*: *LEM* image in a narrow 3 eV interval at the redshifted OVII line (the forbidden component of the triplet, which at this redshift can be resolved from the corresponding Milky Way foreground line as seen in Fig. 7) reveals a “jellyfish” — a trail of cool gas ram-pressure stripped from the infalling galaxy. The hotter group halo does not emit in this line. Such gas tails are a sensitive diagnostic of the plasma physics in galaxy groups and clusters.

echo from past explosions will be seen with a time delay in the fluorescent line emission from the GC molecular clouds.<sup>4</sup> While the bright Fe fluorescent line at 6.4 keV is inaccessible for *LEM*, we will be able to detect such light echo in the Si fluorescence. *LEM* will require only 4–5 pointings to map the entire region of the giant molecular clouds and map the most recent history of activity of our own SMBH.

**Charge exchange emission** in the Jovian magnetosphere, planets and comets. *LEM* will offer revolutionary insights for heliophysics and planetary science. One example is the Jovian system. Jupiter produces the most powerful aurora in the solar system and these are key to understanding which processes govern rapidly-rotating magnetospheres. It is unknown to what extent the X-ray aurora are produced by the precipitation of material that originates in Io’s volcanos or whether they are indicative of the direct entry of solar wind particles into the system<sup>7</sup>.

Figure 14 shows how *LEM*’s exquisite energy resolution will finally solve this problem. The figure shows the unique new access *LEM* provides to

the low energy line emissions from planets. This will open an entirely new paradigm, enabling the bright emissions in this spectral range to be utilized to study previously inaccessible objects or to offer a step change in capability to advance previous X-ray studies of Mars, Saturn, comets, the Ice Giants and the heliosphere<sup>2</sup>.

A possibility to extend the *LEM* calibrated energy band down to  $E = 0.05$  keV is currently under study; while the effective area there would be small, the CX signal at those energies is very luminous. This will also allow diagnostics for species more closely linked to the standard UV lines of CIV, SiIV, NV, and OVI. The sub-eV resolution of *LEM*’s central array would be critical in this very crowded spectral region.

**Earth magnetosphere.** A possibility to point *LEM* toward Earth from an L1 orbit is currently under study. If it is possible, *LEM* will be able to observe the SWCX emission from Earth’s magnetopause and magnetosheath, study their dynamics and their response to the varying solar wind pres-



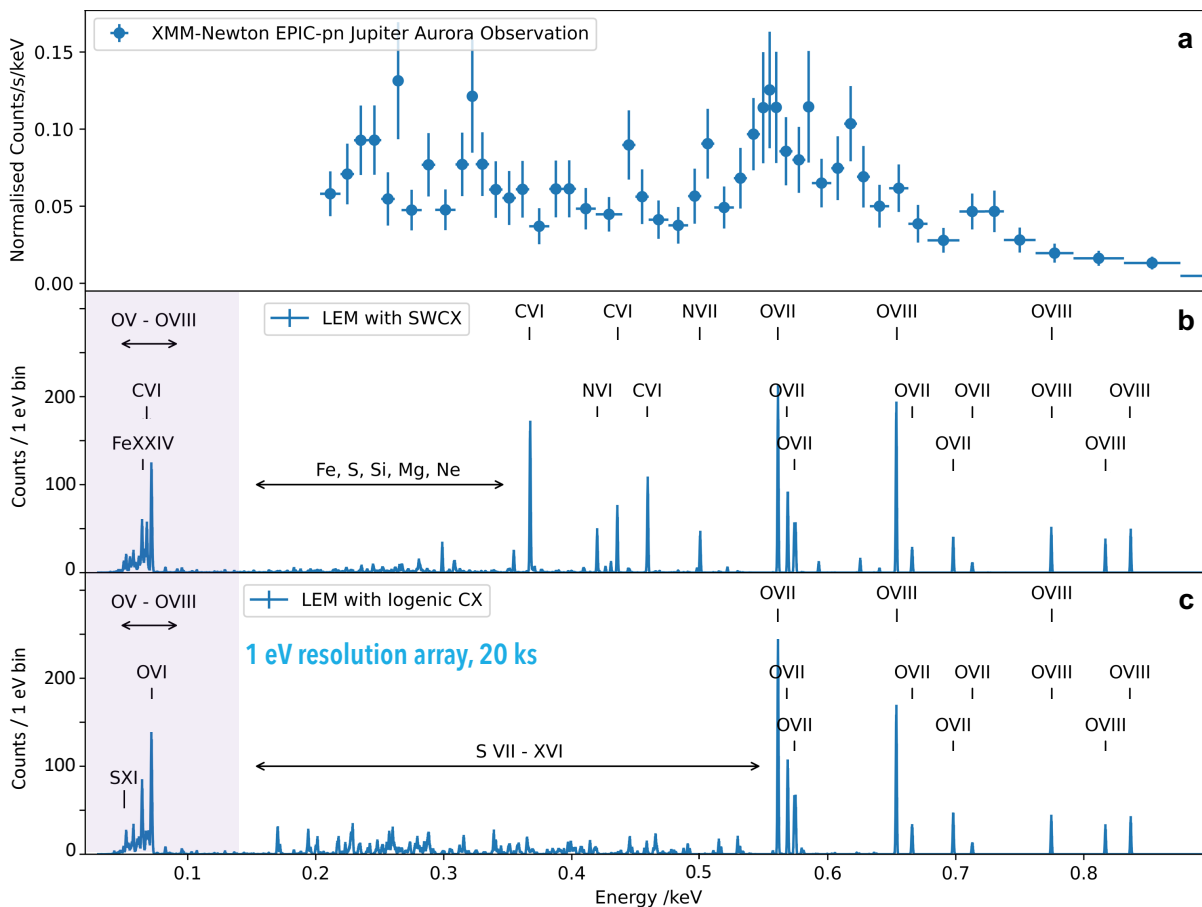


**Fig. 14** — *LEM* will revolutionize solar system studies. (a) *XMM-Newton* EPIC-pn spectrum of Jupiter’s Northern X-ray aurora (130 ks). There are two different models that fit the data well, but each offers fundamentally different explanations for the processes that produce Jupiter’s aurora. The first model is a solar wind charge exchange model (SWCX), implying entrance of solar wind into the Jovian system. The second model is an Iogenic model, which uses charge exchange on the S and O ions from Io’s volcanos. (b,c) *LEM* 1 eV resolution spectra for each scenario. Counts per resolution element for a 20 ks exposure is shown; background is not included for clarity (it is negligible because Jupiter is under  $1'$  in size). The most prominent emission lines are marked. The instrument may offer significant sensitivity at  $E < 0.1$  keV with the same high spectral resolution, providing access to never-before-seen charge exchange lines at low energies (an option currently under study; gray area in the plots). *LEM* will easily distinguish between these models and address key questions on if and when Jupiter’s magnetosphere is open to the solar wind — a point of longstanding debate in the heliophysics and planetary science communities.

sure — a matter of longstanding interest for the heliophysics community.

In addition, the *LEM* observatory will greatly advance the studies of variable black hole winds, flares in exoplanet host stars, protostar accretion rates, interstellar dust in emission and absorption, and numerous other fields. Given the big leap in observing capability that *LEM* will bring, observers will most certainly come up with experiments that

we cannot even foresee at present.

## 4 CONCLUSIONS

The Line Emission Mapper Probe will fundamentally transform our understanding of one of the most important questions in modern astrophysics — the formation of galaxies. The unique ability of this observatory to detect the low surface brightness X-ray emission from the warm and hot gas in galaxy

halos and in the filamentary structures connecting larger mass structures, and to measure the temperature, entropy, and elemental abundances will allow an understanding of the state of this gas that is, at present, only a matter of theoretical speculation. With its combination of wide field of view X-ray optic and energy-dispersive microcalorimeter array, *LEM* offers the opportunity for complete dynamical and thermodynamic characterization of this gas out to a large fraction of the virial radius in Milky Way-sized galaxies and beyond the virial radius for galaxy clusters. *LEM* will detect metals expelled by galaxies over their lifetime and accumulated in the Cosmic Web filaments, and directly measure the imprint of AGN feedback, stellar feedback, and merging over cosmic time in galaxies halos and cluster filaments.

*LEM* is the X-ray mission for the 2030s, and it should be the first of the exciting new line of astrophysics Probes. The primary science of *LEM* is of great interest to the entire astrophysical community, not just the X-ray community. Most of the *LEM* observing time will be dedicated to the guest observer program. The combination of wide field of view and 1–2 eV spectral resolution of the calorimeter offers a unique host of guest observer investigations covering every area of X-ray astrophysics, including studies of AGN, stellar astrophysics, exoplanets, Solar system physics, and time domain and multi-messenger astrophysics. *LEM* also has significant synergies with virtually every ground-based and space-based observatory planned to be in operation in the 2030s, including *SKA*, Roman Space Telescope, *CMB-S4*, and many others. Finally, the technologies required to implement this mission — the lightweight high-resolution X-ray optics and the large microcalorimeter arrays — are rapidly maturing. With small, well-defined, ongoing investments in technology development, *LEM* is already on the path to meet its key mission milestones. *LEM* offers the astrophysics community paradigm-changing science in a Probe package.

1. Ackermann, M., et al. 2014, *ApJ*, 793, 64
2. Bhardwaj, A., et al. 2007, *Planetary & Space Sci.*, 55, 1135
3. Cen, R., & Ostriker, J. P. 1999, *ApJ*, 514, 1
4. Churazov, E., et al. 2017, *MNRAS*, 465, 45
5. Crain, R. A., et al. 2015, *MNRAS*, 450, 1937
6. Davé, R., et al. 2019, *MNRAS*, 486, 2827
7. Dunn, W., 2022, [arXiv:2208.13455](https://arxiv.org/abs/2208.13455)
8. Khabibullin, I. & Churazov, E. 2019, *MNRAS*, 482, 4972
9. Lee, S. J., et al. 2015, *Appl. Phys. Lett.*, 107, 223503
10. Mernier, F., & Biffi, V. 2022, [arXiv:2202.07097](https://arxiv.org/abs/2202.07097)
11. Miniussi, A. R., et al. 2018, *J. Low Temp. Phys.*, 193, 337
12. Nelson, D., et al. 2018, *MNRAS*, 477, 450
13. Nelson, D., et al. 2019a, *Comp. Astrophys. & Cosmology*, 6, 2
14. Nelson, D., et al. 2019b, *MNRAS*, 490, 3234
15. Norris, R. P., et al. 2021, *PASA*, 38, 3
16. Oppenheimer, B. D., et al. 2016, *MNRAS*, 460, 2157
17. Pillepich, A., et al. 2018, *MNRAS*, 473, 4077
18. Pillepich, A., et al. 2019, *MNRAS*, 490, 3196
19. Pillepich, A., et al. 2021, *MNRAS*, 508, 4667
20. Predehl, P., et al. 2020, *Nature*, 588, 227
21. Roediger, E., et al. 2015, *ApJ*, 806, 104
22. Schaye, J., et al. 2015, *MNRAS*, 446, 521
23. Smith, S. J., et al. 2020, *J. Low Temperature Physics*, 199, 330
24. Smith, S. J., et al. 2023, *J. Astron. Telescopes, Instruments, and Systems*, to be submitted
25. Yun, K., et al. 2019, *MNRAS*, 483, 1042
26. ZuHone, J. A., et al. 2016, *ApJ*, 817, 110